Core-scattered combination orbits in the $M=0$ Stark spectrum of helium

M. L. Keeler and T. J. Morgan
Department of Physics, Wesleyan University, Middletown, Connecticut 06459
(Received 28 December 1998)

Scaled-energy spectroscopy is used to measure the $m=0$ Stark recurrence spectrum of the two spin forms of helium. This case is characterized by much stronger orbit-core interaction than the $m=1$ case studied previously. Viewed globally as a function of scaled energy ε and scaled action $\hat{S}$ clusters of core-scattered recurrences are revealed, emphasizing their importance in the Stark spectrum. Data are interpreted using closed-orbit theory. Integrating recurrence peaks over scaled energy allows comparison between singlet and triplet core scattering, highlighting the link with $e+\mathrm{He}^+$ scattering. [S1050-2947(99)04306-1]

PACS number(s): 32.60.+i, 03.65.Sq, 05.45.Mt

The behavior of multielectron atoms in external fields is a fundamental problem in atomic physics. A recent focus in this area is the study of relationships between quantum spectra and the classical dynamics of nonhydrogenic Rydberg atoms, especially in systems exhibiting chaos [1]. The helium atom is the prototypical quantum atomic system whose underlying classical dynamics is chaotic, induced by core scattering. It has been predicted that $e^-+\mathrm{He}^+$ scattering exhibits Ericson fluctuations that serve as a signature of chaos [2]. A recent theoretical study of the spectral characteristics of nonhydrogenic atoms in electric fields shows that the ionic core induces unusual statistical properties, attributable to neither regular nor chaotic systems [3].

To date there have been only two experimental studies of recurrences (electron waves that go from and return to the atomic core) in the Stark spectrum of helium [4,5]. Using constant-scaled-energy spectroscopy both studies investigated $m=1$ Rydberg states which produce combination recurrences (nonhydrogenic recurrences that are combinations of hydrogenic orbits) that have closed classical orbits with actions very close to hydrogen, producing changes mostly to the intensity of peaks that already exist in the spectrum of hydrogen. For example, Keeler and Morgan observed pronounced modulations in intensity in the triplet spectrum of helium due to interference between hydrogenic and combination recurrences [4].

In the present work, we report results of an experimental study of the recurrence spectrum of $m=0$ Rydberg states of helium in an electric field. Recurrences are more numerous and complex in this case due to enhanced diffraction on the atomic core. The experiment reveals the presence of peaks not present in hydrogen nor in $m=1$ helium states that depend strongly on the spin state ($S=0$ or 1) of the scattering system. The peaks, due to scattering of the Rydberg electron by the helium ionic core in the absence of an angular momentum barrier, result in combination orbits with actions far from hydrogen. In the case of triplet states with an s-state quantum defect of $\delta_0^t=0.3$, the scattering is abundant in particular areas of the recurrence map [$(\varepsilon,\hat{S})$ space]. Although still similar to hydrogen in many ways, the scattering produces a radically different recurrence map in certain regions of $(\varepsilon,\hat{S})$ space that are effectively populated by core-scattered combination peaks and devoid of large hydrogenic peaks.

The quantum and classical manifestations of the core of a Rydberg atom in an electric field and their incorporation into semiclassical closed-orbit theory are under active investigation. It was pointed out by Gao and Delos that a nonhydrogenic core produced scattering from one hydrogenic closed orbit into another [6]. Recent work on $m=0$ states has extended closed-orbit theory to scattering in the presence of bifurcations [7]. Scattering recurrence peaks have been observed experimentally in $m=0$ Stark states of lithium [8] and in diamagnetic helium [9]. Theoretical activity to explain these peaks has used both a semiclassical approach employing quantum defect theory [10] and a purely classical approach using a model potential [11] to describe the core scattering. The classical analysis has revealed that core scattering creates a large number of new clusters of closed orbits that interfere to produce novel structure in recurrence spectra. The quantum defect method extends closed-orbit theory to include core-scattered waves and it shows good agreement with full quantum calculations. A third approach, emphasizing the effects of avoided crossings, provides new insight into the main differences between hydrogen and helium recurrence maps [12].

Closed-orbit theory takes advantage of properties of the hydrogen Hamiltonian in an external field by the application of a set of scaled variables [6]. This leads to a Hamiltonian in which the electron energy E and external electric field F are replaced by a single parameter $\varepsilon=E/\sqrt{F}$, the scaled energy. By scanning the excitation energy while maintaining a con-

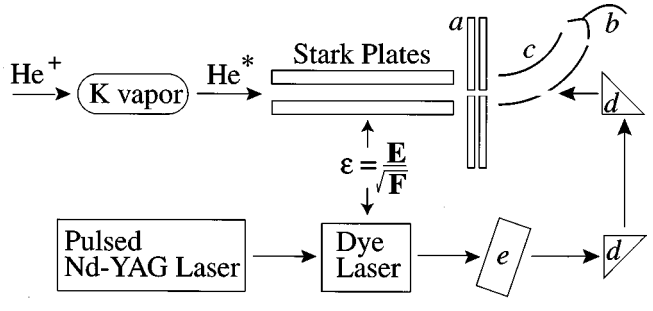

FIG. 1. Constant-scaled-energy Stark spectroscopy apparatus. Computer control of laser wavelength and Stark field maintains a constant scaled energy ε. The interaction region extends over the 37-cm length of the Stark plates. (a) Field ionizer, (b) channeltron, (c) electrostatic deflectors, (d) quartz prism, (e) doubling crystal.

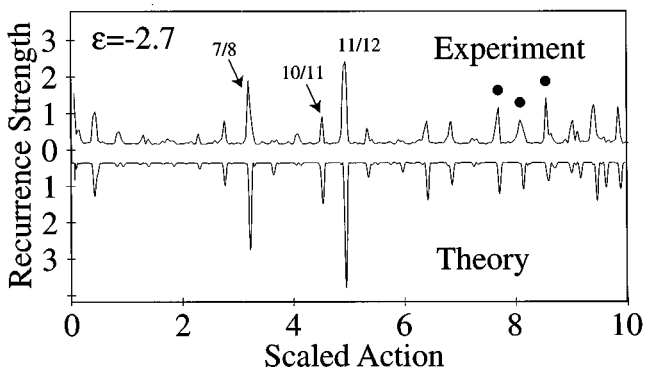

FIG. 2. Mirror plot of $20<n<30$ experimental triplet helium, $m=0$, $\varepsilon=-2.7$ recurrence spectra with quantum theory [7] on bottom. Black dots identify core-scattered nonhydrogenic peaks.

stant scaled energy individual trajectories contribute a sinusoidal spectrum in which each individual peak at a scaled action represents a closed classical trajectory at a particular scaled energy. Each trajectory returns to the core, giving it the opportunity to interfere with other orbits. Quantum mechanical wave fronts can be constructed from the returning trajectories and take on the primitive form $R_k = C_k e^{i(2\pi S_k+\Delta_k)}$, where C_k is the classical amplitude and the total phase is determined by the action of the orbit S_k and a constant Δ_k, unique to the orbit. For two peaks with nearly the same action, interference is possible and the total recurrence strength is given by the coherent sum. Combination core-scattered orbits are due to a hydrogenic orbit scattering into another in a small region near the nucleus. They are composed of two (or more) actions and have an amplitude R_{jk} proportional to the amplitudes of the parent orbits and the scattering amplitude $A_{j,k}$ from one orbit into another, $R_{jk}=A_{j,k}C_jC_ke^{i(2\pi[S_j+S_k]+[\Delta_j+\Delta_k])}$. Each closed classical trajectory or scattered combination orbit has a characteristic action, amplitude, and phase upon returning to the core region. It is this information which allows interpretation of scattered resonances in a nonhydrogenic recurrence spectrum.

Recently, we reported the effect of core-scattered combination orbits in $m=1$ states of helium in terms of specific closed orbits [4]. In the present work, the clustering and complex composition of $m=0$ recurrence peaks prevents a simple analysis as a function of orbit type. Instead, we study core scattering in regions of $(\varepsilon,\hat{S})$ space with high scattered combination orbit strength and low hydrogenic strength. These densely populated regions are due to several scattered combination orbits clustering at about the same scaled action. Integrating in $(\varepsilon,\hat{S})$ space over high probability regions allows us to interpret the results as a function of average cluster location and provides a comparison of overall $e^-+\mathrm{He}^+$ core scattering strength between singlet and triplet states.

A diagram of the apparatus is shown in Fig. 1. Helium ions are created in an ion source, accelerated to 4 kV and selected by a velocity filter. The beam is neutralized in a potassium charge exchange cell, with the metastable $2s\,^1S$ and $2s\,^3S$ states efficiently populated. Excitation to a Rydberg-Stark state takes place between field plates 37 cm long separated by 1 cm. Laser light from a pulsed YAG (yttrium aluminum garnet) laser pumps a dye laser whose output is sent through a doubling crystal to generate tunable UV light. The laser is aligned antiparallel to the helium beam, and excites Rydberg-Stark states in the $n=20$–30 range. The m state is experimentally defined by the orientation of the Stark plates with respect to the laser polarization. After the Stark plates, a field of 7.0 kV cm^{-1} oriented along the beam ionizes excited atoms with the resulting He^+ ions detected by a channeltron. The ion signal is amplified and averaged over ten laser pulses. To maintain a constant scaled energy, the computer continuously monitors the laser wavelength and adjusts the Stark field while recording the ion

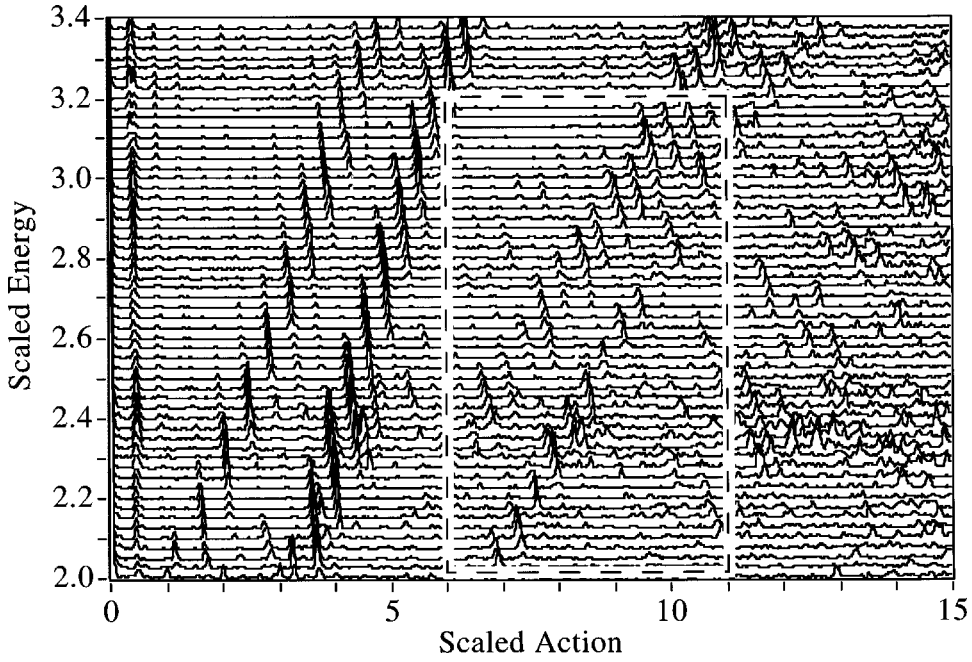

FIG. 3. Recurrence map for triplet helium $m=0$ states composed of 56 measured constant-scaled-energy spectra. The dotted outline contains strong core-scattered combination recurrences and encloses the range for the contour maps shown in Fig. 4.

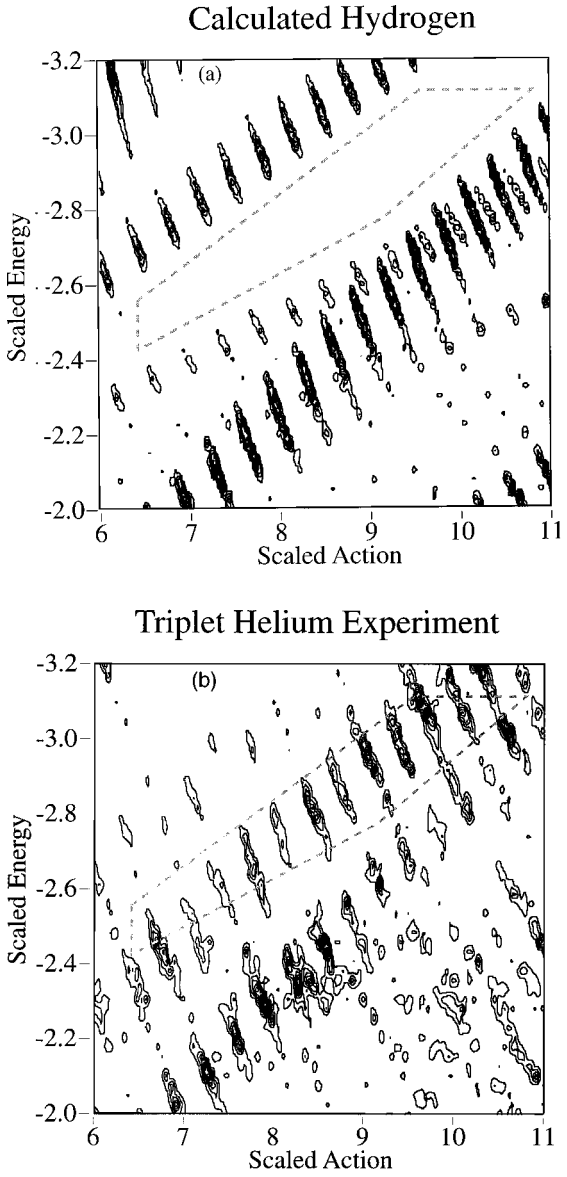

FIG. 4. Recurrence contour maps for (a) calculated hydrogen, (b) measured triplet helium. The dotted region lies between downhill and uphill sequence-2 orbits and defines a region of low hydrogenic activity used to investigate scattering and combination orbits. In helium, combination orbits cluster to form high amplitude recurrences in this region.

signal. For a particular scaled energy, data are recorded as a function of the scaled parameter $F^{-1/4}$ and Fourier transformed to give a recurrence spectrum.

Figure 2 shows an example of our measured $m=0$ triplet helium constant-scaled-energy recurrence spectrum in a mirror plot with a quantum calculation [7]. A uniform semiclassical calculation is in good agreement with the quantum calculation [7], verifying the use of the semiclassical theory to explain our results. Small differences between theory and experiment exist (due in part to uncertainties in the value of the scaled energy) but overall agreement is good. To interpret resonances, trajectories are calculated in semiparabolic coordinates (u,v) where $u^2=r+z$ and $v^2=r-z$, with the external electric field defining the direction of the z axis. Three trajectories are labeled in Fig. 2. They are identified by their period ratio τ_u/τ_v, the ratio of oscillations in (u,v)

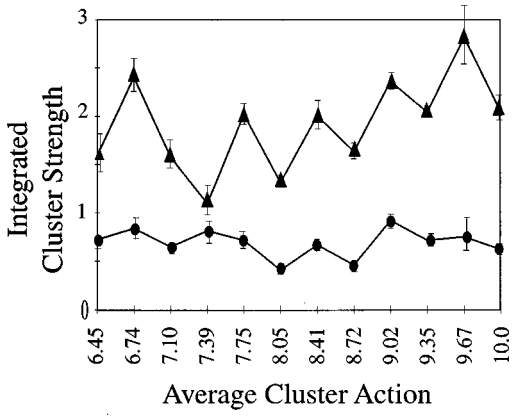

FIG. 5. Cluster integrated recurrence strength (from Fig. 4) versus average cluster scaled action. Triangles refer to triplet helium and dots refer to singlet helium.

space [8,13]. Strong core-scattered combination orbit peaks are indicated by solid dots, and do not exist in hydrogen. Recurrence strength scatters out of low action peaks into combination orbits with actions equal to the sum of the scattering partners. For example, the peaks at $\hat{S}=3.65$ and 4.52 suggest that orbits with period ratios 8/9 and 10/11 are combining to contribute to the peak at $\hat{S}=8.17$. Additionally, a large combination orbit peak at $\hat{S}=8.15$ results from orbits 7/8 and 11/12 and is not resolvable from the $\hat{S}=8.17$ peak. In order to characterize the scattering strength of a particular cluster of combination orbits, we measure recurrence spectra over the allowed scaled-energy range of the orbits and integrate the orbit recurrence peaks in the spectra. This permits a comparison of the overall scattering strength of different combination orbit clusters and allows a global comparison between triplet and singlet scattering systems.

To achieve this, 56 spectra were measured between $\varepsilon=-2$ (ionization threshold) and -3.4 in steps of 0.025 for singlet and triplet helium. By consolidating the spectra into a single plot called a recurrence map we create a three-dimensional picture of orbit probability as a function of ε and $\hat{S}$. Figure 3 shows our measured recurrence map for $m=0$ triplet states. There are four clear bands cutting through the map. The first two (reading from left to right) are downhill and uphill orbits, respectively, with period ratios given by $i/(i+1)$ and referred to as the first sequence. The fourth band contains uphill orbits with period ratio $i/(i+2)$. (Corresponding downhill orbits in the second sequence are reduced in strength due to core scattering and are not as obvious in the figure. In singlet helium and hydrogen this downhill band is more pronounced.) The third strong band is the result of core scattering. It appears in the map between downhill and uphill orbits of the second sequence and comes primarily from combinations of orbits of the two bands in the first sequence. It is a consequence of the structure of the first two orbit bands in the map and should manifest itself in other nonhydrogenic atoms. Hot spots appear at many locations in the map due to constructive interferences between bifurcated orbits and combination orbits. The dotted rectangle frames the region of interest and the boundary of the recurrence maps shown in Fig. 4. These maps consist of two contour-style recurrence plots; calculated hydrogen [Fig. 4(a)] and

measured triplet helium [Fig. 4(b)], over the range $6<\hat{S}<11$ and $-3.2<\varepsilon<-2$. The hydrogen map shows a distinct low intensity region (interior of the dotted outline) between the second sequence downhill and uphill orbits. This is due to the initial shape of the outgoing waves produced by the laser whose amplitudes are proportional to the Legendre polynomial $Y_1^0(\theta)$ where θ is the launching angle measured from the external field axis. When the laser is oriented along the field to produce $m=0$ states each hydrogenic closed orbit has an increased amplitude for launching angles near 0 (uphill) or π (downhill) while launching angles near $\pi/2$ have almost no amplitude. In hydrogen, only orbits with initial launching angles near $\pi/2$ have actions that fall within the region defined by the dotted lines. Hydrogen parallel repetition orbits fall within this region for $m=0$, but they are relatively weak and not observable on the scale of Fig. 4(a). In the case of helium, we have found that core scattering combination orbits have substantial recurrences in this region [Fig. 4(b)].

Combination orbits are formed when the returning wave front of a classical trajectory diffracts off a nonhydrogenic core. The diffracted wave front diverts electron probability to the initial conditions required to launch new trajectories. In hydrogen, for near-zero energies, the wave front simply reflects backwards, forming an identical orbit in reverse, producing an orbit repetition. For a nonhydrogenic core the diffracted wave redirects probability to other orbits, creating combination orbits composed of two trajectories which scatter one into another to form a new orbit whose action is the sum of the parent orbits. The amplitudes and phases of orbits determine how trajectories contribute to the nonhydrogenic peaks.

Incorporation of bifurcation theory with core scattering into closed-orbit theory of $m=0$ states has recently been achieved, and the closed-orbit calculations aid interpretation of our data [7,14]. In general, there are several significant combination orbits, both on axis and off axis, associated with each nonhydrogenic cluster. Examples of strong single collision scattering combinations include orbits from the first two bands with period ratios $i/(i+1)\oplus(i+2)/(i+3)$, $i/(i+1)\oplus i+3/(i+4)$, and $i/(i+1)\oplus(i+4)/(i+5)$, where $\oplus$ indicates core scattering from one hydrogenic orbit into another. Smaller amplitude combination orbits are produced from unstable orbits or orbits whose initial launching angles are weakly populated in $m=0$ excitation. As the scaled action increases the number of closed-orbit contributions increases dramatically, making the recurrence peaks a delicate function of the exact scaled energy since the sum of many contributions is very sensitive to phase. A complete understanding of the physics of $m=0$ core-scattered combination recurrences is at present not available and remains a challenge to theory.

To study the amplitude of the combination orbits, it is convenient to use the notion of integrated recurrence strength, introduced in Ref. [4]. The integration region is chosen visually to contain high recurrence strength associated with scattered clusters and is shown in Fig. 4. The result of this procedure is a measure of total recurrence strength versus average cluster scaled action (Fig. 5). Figure 5 shows distinct strength variation with cluster location in the triplet spectrum. There is variation in strength in the singlet case also, only less distinct because of the weaker scattered signal, consistent with a smaller quantum defect of $\delta_0^s=0.14$. Error bars were generated by accounting for variations resulting from the choice of the integration boundary range.

The Rydberg helium system can be modeled as a spin polarized scattering experiment. For weak scattering, the leading term in a partial wave analysis of the total cross section is proportional to the square of the phase shift of the wave front. The phase shift is proportional to the quantum defect and therefore the ratio $(\delta_0^t/\delta_0^s)^2$, which equals 4.6 in the present case, is an approximate measure of the relative scattering strength of the two spin states of Rydberg helium atoms. For the eight complete interior clusters measured, and shown in the nonhydrogenic region in Fig. 4, the average ratio of triplet to singlet integrated intensity is 3.3 ± 0.4. Direct comparison with $e^-+\mathrm{He}^+$ scattering requires taking account of the contribution of the nonscattered background in the recurrence maps which will increase the value of the measured ratio. This requires detailed knowledge not presently available of the amplitude and phase of all scattered and non-scattered recurrences. Estimating the correction gives 5 ± 1 for the ratio.

In summary, closed-orbit theory has been used to interpret the measured recurrence spectrum of singlet and triplet helium $m=0$ Rydberg-Stark states. In contrast to $m=1$ states, core scattering introduces many extra peaks in the spectrum. Studying combination orbits in a region of the recurrence map devoid of large hydrogenic peaks has allowed us to identify core effects in terms of clusters of combination orbits and to investigate scattering probability as a function of combination orbit cluster location in $(\varepsilon,\hat{S})$ space. We observe modulations in the recurrence spectra versus scattering cluster and a strong combination-orbit-production spin-state dependence. Also, the measured triplet/singlet ratio of core-scattered orbit recurrences averaged over an extended nonhydrogenic region in $(\varepsilon,\hat{S})$ space is consistent with $e^-+\mathrm{He}^+$ scattering of $l=0$ partial waves, highlighting the link between electron-ion scattering and Rydberg spectra.

Note added in proof. Recently, the $m=0$ Stark spectrum of helium has been measured at two scaled energies ($\varepsilon=-2.94$ and -2.35) for $n=55$ to 80 [15]. The data are interpreted using closed-orbit theory and small nonhydrogenic peaks are attributed to core scattering.

We thank R. Jensen, V. Kondratovich, and J. Shaw for valuable discussions, and J. Shaw for helium quantum calculations. Thanks are due to H. Flores for help in the laboratory and D. Wright for help with data analysis. This work was supported by the National Science Foundation.

[1] T. S. Monteiro and G. Wunner, Phys. Rev. Lett. **65**, 1100 (1990).

[2] R. Blümel and W. P. Reinhardt, *Chaos in Atomic Physics* (Cambridge University Press, Cambridge, England, 1997).

[3] T. Jonckheere, B. Gremaud, and D. Delande, Phys. Rev. Lett. **81**, 2442 (1998).

[4] M. Keeler and T. J. Morgan, Phys. Rev. Lett. **80**, 5726 (1998).

[5] A. Kips *et al.*, Phys. Rev. A **58**, 3043 (1998).

[6] J. Gao and J. B. Delos, Phys. Rev. A **46**, 1455 (1992).
[7] J. A. Shaw and F. Robicheaux, Phys. Rev. A **58**, 3561 (1998).
[8] M. Courtney *et al.*, Phys. Rev. A **51**, 3604 (1995).
[9] B. Hupper, J. Main, and G. Wunner, Phys. Rev. Lett. **74**, 2650 (1995).
[10] P. A. Dando *et al.*, Phys. Rev. A **54**, 127 (1996).
[11] B. Hupper, J. Main, and G. Wunner, Phys. Rev. A **53**, 744 (1996).
[12] R. V. Jensen, M. L. Keeler, and T. J. Morgan, Bull. Am. Phys. Soc. **44**, 140 (1999).
[13] J. Gao, J. B. Delos, and M. Baruch, Phys. Rev. A **46**, 1449 (1992); J. Gao and J. B. Delos, *ibid.* **49**, 869 (1994).
[14] J. Shaw (private communication); F. Robicheaux and J. Shaw, Phys. Rev. A **56**, 278 (1997).
[15] A. Kips, W. Vassen, and W. Hogervorst, Phys. Rev. A **59**, 2948 (1999).